Electromagnetically Induced Transparency Cooling

ECE 522: Quantum Engineering with Atoms

Maanav Allampallam, Ishan Vyas

April 2025

1 Introduction

Atomic cooling is a foundational concept in quantum information science and a necessary capability for any system that traps neutral atoms or ions. Cooling atoms increases the efficiency of the traps, as it reduces the probability of the particle jumping out of the trap (especially necessary for shallow traps like Paul or Penning traps). Cooling also reduces thermal noise, which increases coherence times and qubit stability.

2 Doppler Cooling

Doppler cooling was the first cooling technique which could get close to the temperatures required for atom/ion trapping systems. The basic idea is to use a laser to impart a momentum kick on the atom moving in a direction to reduce its momentum in that direction, thereby reducing its overall kinetic energy[1]. To ensure the momentum kick only happens in that direction, the laser is red-detuned from the resonant frequency. When the atom moves in the direction opposite to the laser propagation, the Doppler shift raises the frequency to resonance, allowing for photon absorption. However, the absorbed photon is eventually emitted. While this emission is isotropic [1], meaning there is no momentum change, it does add kinetic energy to the atom. Hence, there is an equilibrium between the cooling from the absorption and heating from the emission. The temperature at this equilibrium is the coldest Doppler cooling can make a system. Below is a brief derivation based on [1] of this lower limit, as Doppler cooling is not the primary focus of this report.

We define the cooling force on the laser as

$$F_c = \hbar k \Gamma \rho_{\pm}$$

where $\hbar k$ is the momentum of the absorbed photon and the $\Gamma\rho_{\pm}$ is the scattering rate. $\rho_{\pm}$ is the excited state population and can be derived from solving the Optical Bloch equations.

$$\rho_{\pm} = \frac{I/I_{sat}}{2(1 + I_{sat} + 4\frac{(\delta \mp kv)^2}{\Gamma^2})}$$

The $\pm$ is positive if the atom is traveling against the laser, and negative if it is traveling with the laser.

We define the energy added through emission as

$$E_e = \frac{(\hbar k)^2}{2m}$$

This is simply the kinetic energy of the photon.

Now consider a 1D system with lasers shining to the right and left and a two-level atom moving to the right. Below are the net cooling force, net cooling rate R_c, and net heating rate R_H.

$$\sum F_c = \hbar k\Gamma(\rho_+ - \rho_-)$$

$$R_c = (\sum F_c)v$$

$$R_H = \frac{(\hbar k)^2}{2m}\Gamma((\rho_+ - \rho_-)$$

By setting $R_c = R_H$, applying the equipartition theorem $\frac{1}{2}mv^2 = \frac{1}{2}k_BT^2$, and doing some algebra, you get the following as the Doppler limit.

$$T_D = \frac{\hbar\Gamma}{2k_B}$$

In practice, this temperature is usually around a few hundred microkelvin. While this is very cold, quantum computing gates require coherence times for which even a few hundred microkelvin is too high. To bypass this limit, we use EIT cooling.

3 Theory of EIT Cooling

3.1 EIT Principles and Setup

Multi-level atomic systems demonstrate transparency when specific wavelengths of lasers are applied. This transparency effect relies on quantum interference to function, using the interference to prevent transitions into an excited state.

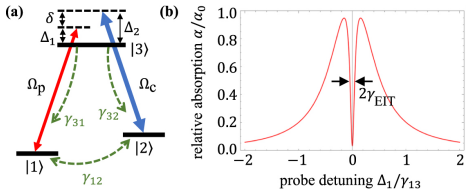

Figure 1: Finkelstein et al, 2023. a) A typical 3-level Λ system is shown, with probe laser Ω_p and control laser Ω_c shown. b) Demonstration of transparency effect for select wavelength and detunings.

As a result, electrons become 'transparent' to light, as the interference prevents absorption. This transparency effect is the foundation that allows EIT cooling to work.

The system setup is as follows. EIT relies on the existence of a Λ 3-state configuration, where there exists two stable or metastable states $|f\rangle$ and $|g\rangle$ and an excited state $|e\rangle$. An example of this configuration is in $^{40}Ca^{+}$, where two $S_{1/2}$ Zeeman sublevels comprise the stable states $|f\rangle$ and $|g\rangle$ and one of the $P_{1/2}$ Zeeman sublevels represents the excited state [2].

Figure 1 demonstrates a typical configuration, complete with laser/state detuning Δ_n and slight probe/control detuning δ [3]. In the figure, γ_{31} and γ_{32} represent the rate of spontaneous emission from state i to state j.

3.2 Dressed States

The application of a strong controlled laser creates a phenomenon called 'dressed states'. Dressed states are a result of the Autler-Townes Effect, also known as the AC Stark Effect. When the strong coupling laser is turned on, the atom-light interaction between the laser and the $|g\rangle$ and $|e\rangle$ states changes the eigenstates of the Hamiltonian [4]. Without covering the mechanisms by which this state shift occurs, we get that the states shift away from each other by an amount δt, where the 'ground' state rises and the excited state lowers. Figure 2 illustrates the state dressing in a 3-level system [5]. The resulting state shift is calculated as:

$$\delta t = \frac{1}{2}(\sqrt{\Omega_c^2 + \Delta_c^2} - |\Delta_c|)$$

These new shifted states are represented by $|\tilde{g}\rangle$ and $|\tilde{e}\rangle$. Though we will discuss motional sidebands later, it should be noted that the dressed $|\tilde{g}, n-1\rangle$ state will almost exclusively decay into the $|f, n-1\rangle$ state, so long as the system is within or near the Lamb-Dicke regime [6]. This condition can be proved by examining the expansion of the recoil operator:

$$e^{i\eta(a+a^\dagger)} \approx 1 + i\eta(a + a^\dagger) + \mathcal{O}(\eta^2)$$

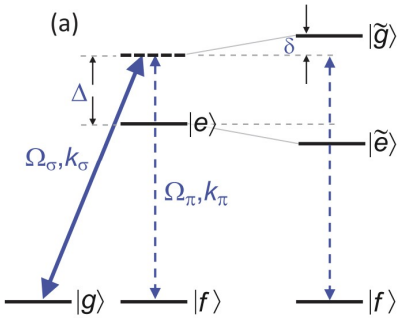

Figure 2: Lechner et al, 2016. Dressed states in a 3-level Λ system

In this case, for $\eta << 1$, the coefficients of the raising/lowering operators are about 0, meaning the chance of emission changing the motional state of the electron is near 0.

Viewing the equation for the state dressing δt, we can see that tuning the Rabi frequency and detuning of the control laser gives precise control over the energy eigenstates. This precise state control enables electromagnetically induced transparency to occur by placing the excited state in the dark spot of the Fano-type profile, explained in the sections below.

3.3 Dark States

So far, we have strictly considered the implementation of the coupling laser (ω_c, Ω_c) between the stable state $|g\rangle$ and the excited state $|e\rangle$. Let's now include a weaker probe laser with natural frequency ω_p and Rabi frequency Ω_p, set between the metastable state $|f\rangle$ and the excited state $|e\rangle$. As derived in Lambropoulos and Petrosyan [7], for this example, we will not include any detuning. We want to analyze the effect of the interaction between the atom and the incoming lasers. The Hamiltonian of the system is straightforward:

$$H_0 = \hbar\omega_g |g\rangle \langle g| + \hbar\omega_f |f\rangle \langle f| + \hbar\omega_e |e\rangle \langle e|$$

The atom-light interaction Hamiltonian is a separate topic of discussion, and is derivable via the rotating wave approximation; it is equal to:

$$H'(t) = -\frac{\hbar}{2}[\Omega_c e^{-i\omega_c t} |e\rangle \langle g| + \Omega_p e^{-i\omega_p t} |e\rangle \langle f|] + h.c.$$

We set up the time-dependent Schrödinger equation, giving:

$$i\hbar\frac{\partial}{\partial t} |\Psi(t)\rangle = [\hat{H}_0 + \hat{H}'(t)] |\Psi(t)\rangle$$

$$|\Psi(t)\rangle = c_g(t)\,|g\rangle + c_f(t)\,|f\rangle + c_e(t)\,|e\rangle$$

Using time-dependent perturbation theory, we can arrive at equations that describe the time evolution of the states. Those equations are:

$$c_g(t) = c_g(0)\left[\frac{\Omega_c^2}{\Omega^2} + \frac{\Omega_p^2}{\Omega^2}\cos\left(\frac{\Omega t}{2}\right)\right] + c_f(0)\left[-\frac{\Omega_p\Omega_c}{\Omega^2} + \frac{\Omega_p\Omega_c}{\Omega^2}\cos\left(\frac{\Omega t}{2}\right)\right] - ic_e(0)\frac{\Omega_p}{\Omega}\sin\left(\frac{\Omega t}{2}\right)$$

$$c_f(t) = c_g(0)\left[-\frac{\Omega_p\Omega_c}{\Omega^2} + \frac{\Omega_p\Omega_c}{\Omega^2}\cos\left(\frac{\Omega t}{2}\right)\right] + c_f(0)\left[\frac{\Omega_p^2}{\Omega^2} + \frac{\Omega_c^2}{\Omega^2}\cos\left(\frac{\Omega t}{2}\right)\right] - ic_e(0)\frac{\Omega_c}{\Omega}\sin\left(\frac{\Omega t}{2}\right)$$

$$c_e(t) = -ic_g(0)\frac{\Omega_p}{\Omega}\sin\left(\frac{\Omega t}{2}\right) - ic_f(0)\frac{\Omega_c}{\Omega}\sin\left(\frac{\Omega t}{2}\right) + c_e(0)\cos\left(\frac{\Omega t}{2}\right)$$

noting that $\Omega = \sqrt{\Omega_p^2 + \Omega_c^2}$. More important than the time evolutions themselves is the fact that we can choose a starting state of:

$$|D\rangle = \cos(\theta)\,|f\rangle - \sin(\theta)\,|g\rangle$$

of which $\tan(\theta) = \frac{\Omega_p}{\Omega_c}$, where the time evolution into the third state, $c_e(t)$, is always equal to 0. This occurs because the $c_f(0)$ and $c_g(0)$ terms become out of phase by π and cancel out. Physically, this effect is called quantum interference, where the excitation of the $|g\rangle$ and $|f\rangle$ states interfere with each other and prevent either excitation. In other words, once the electron reaches the dark state, it cannot evolve into the excited state. The electron becomes 'transparent', where the light passes through without interacting with the electron. For this reason, we call $|D\rangle$ the dark state.

A tangential argument can be made for the state $|B\rangle$, defined as the orthogonal state to $|D\rangle$. For the dark state above, we can find:

$$|B\rangle = \sin(\theta)\,|f\rangle + \cos(\theta)\,|g\rangle$$

In the state $|B\rangle$, transition into the excited state is at a maximum; as a result, this state is called the 'bright' state.

3.4 Fano Profile

We return to our 3-level Λ system with dressed states and probe and control laser detunings. A result of electromagnetically induced transparency is the existence of a Fano profile, shown in the top right of Figure 3. A Fano profile measures the absorbance of a particular state for various laser detunings, and it

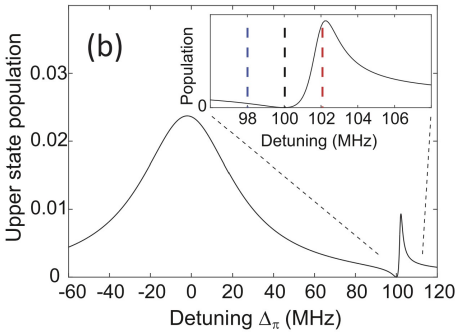

Figure 3: Lechner et al, 2016. Fano-type profile across variable detuning

is characterized by a thin band of near-zero absorbance. This region of minimal absorbance corresponds to the dark state discussed above; a similar maximum absorbance corresponding to the bright state is slightly further detuned from the dark state.

For EIT cooling, our goal is to engineer the system such that the excited state is in this narrow region of minimal absorbance and for the lower motional sideband of the excited state, represented by $|e, n-1\rangle$, to be in the bright state. In this case, we would have maximum absorbance into the lower motional sideband, and due to our system being in the Lamb-Dicke regime, we would reach a lower motional ground state. That setup is shown in Figure 3, where the red dashed line corresponds to the lower motional sideband, and the blue dashed line corresponds to the higher sideband [5].

3.5 Multi-Ion Chains

EIT Cooling is particularly useful for cooling multi-ion chains; ignoring the lasers needed to set up the Λ configuration, just two lasers are needed to cool any N chain of ions. The reason for why this is true relies on our picture of the Fano profile in Figure 3. For cooling to work, we need two conditions to be true. First, the red sideband needs to exist somewhere along the enhanced section, close to but not necessarily exactly on the bright state. Second, the excited state of the same motional sideband must be aligned with the dark state. Given those conditions, we do not need to address each individual sideband frequency; we can instead address all sidebands at once. It is implied that all ions in the chain have a relatively similar motional mode at the start of the cooling process; if not, then our laser could not address ions effectively. Chains of up to 40 atoms at once have been cooled using EIT methods, though more are theoretically possible [8].

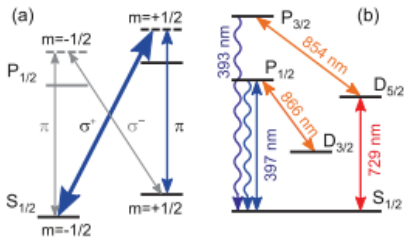

Figure 4: Adapted from Lechner et al, 2016. a) Laser beams and cooling transitions b)$^{40}Ca^{+}$ transitions used in experiment

4 Experimental Cases

The main advantage of EIT cooling is its ability to simultaneously cool many ions. As such, we will examine two experimental setups from Lechner et al. in which long chains of ions were cooled. Lechner et al. built two EIT cooling setups and used them to simultaneously cool the radial modes of 9 to 18 $^{40}Ca^{+}$ ions. Both setups used the $S_{1/2} \leftrightarrow P_{1/2}$ (397nm) as the cooling transition, the $D_{3/2} \leftrightarrow P_{1/2}$ (866nm) as the repump, $D_{5/2} \leftrightarrow P_{3/2}$ (854nm) as the quench, and finally $S_{1/2} \leftrightarrow D_{5/2}$ (729nm) as the clock frequency (used for sideband analysis post cooling). Figure 4b. shows a diagram of the energy transitions. The cooling laser was a diode laser, and the beam was split to create the dressing and probe beams.

4.1 Setup 1

Setup 1 utilized a macroscopic linear RF trap. A magnetic field of .4mT was used to create an 11.4 MHz Zeeman splitting. Finally, the dressing beam was blue detuned by 106MHz.

4.2 Setup 2

Setup 2 utilized a microfabricated segmented surface trap with a segment length of 250μm. A magnetic field of .33mT was used to create a 9.3MHz Zeeman splitting. The dressing beam was detuned by 105MHz.

4.3 Procedure

1. Doppler cool for a few milliseconds
2. EIT cool for 1ms
3. Analyze with sideband spectroscopy

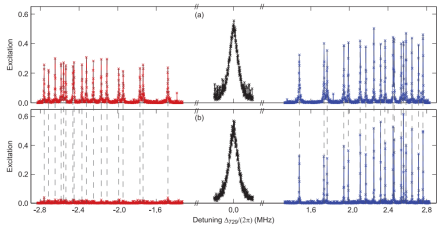

Figure 5: Adapted from Lechner et al, 2016. Top is after Doppler Cooling. Bottom is after EIT. Absense of red sidebands after EIT verifies ground state cooling

4.4 Results and Shortcomings

Ground state cooling was achieved with less than 1ms cooling times in both setups for both 9 and 18 ions (18 and 36 radial modes, respectively). n was less than 1 by at least two orders of magnitude in Setup 1 and one order of magnitude less than 1 in Setup 2. The best cooling rates achieved by Setup 1 and 2 were 19kHz and 17kHz, respectively. In both setups, ground state cooling was verified by analyzing the sidebands. Figure 6. shows the before and after for the 9 ion chain. Although not the goal of the experiments, there was observed heating of the axial modes in both setups. The authors attribute this to the nonzero projection of the Raman k-vector onto the axial direction combined with the fact that the axial modes were not in the Lamb-Dicke regime after Doppler cooling. This caused increased photon scattering leading to heating. They also mentioned polarization impurities. These impurities could cause unwanted transitions, break dark state coherence, and increase uncontrolled scattering.

4.5 Combination Technique

A fundamental shortcoming of the EIT cooling concept is that, since it is a fast broadband technique, it lacks the precision of other side band cooling techniques. However, there is nothing stopping researchers from combining these techniques. Feng et al. used a "tripod" EIT cooling scheme to quickly cool down the 36 atoms in their chain at a 3MHz cooling bandwidth, and then used mode-selective resolved sideband cooling for more precision. With this, they were able to achieve ground-state cooling in less than 300 μs for ion chains of up to 40 atoms.

5 Future Outlook

EIT cooling is one of the most promising cooling technologies for quantum computing. Its scalability and robustness make it perfect for quantum computing applications that require many gates. The trend in the literature has been towards more ions and larger cooling bandwidths, so it is very possible that EIT cooling becomes the universal first-stage cooling for quantum computers

(followed by more precise methods like mode-selective RSB cooling). Companies like IonQ and Quantinium are trying to further increase the scalability by reducing the optical setup through on-chip EIT beam routing. Researchers at Harvard-CFA have also begun to utilize EIT cooling for molecules and nanoparticles, expanding its applications beyond the field of quantum computing. Overall, this is a very exciting technology with a bright future.

6 Author Contributions

Sections 1, 2, 4 and 5 of this paper were primarily researched for and written by Maanav Allampallam, and section 3, the bulk of EIT theory, was written by Ishan Vyas.

References

[1] S. Stenholm, "The semiclassical theory of laser cooling," *Rev. Mod. Phys.*, vol. 58, no. 3, pp. 699–739, 1986.

[2] C. F. Roos, D. Leibfried, A. Mundt, F. Schmidt-Kaler, J. Eschner, and R. Blatt, "Experimental demonstration of ground state laser cooling with electromagnetically induced transparency," *Physical Review Letters*, vol. 85, no. 26, pp. 5547–5550, 2000.

[3] R. Finkelstein, S. Bali, O. Firstenberg, and I. Novikova, "A practical guide to electromagnetically induced transparency in atomic vapor," *New Journal of Physics*, vol. 25, 2023.

[4] P. M. Anisimov, J. P. Dowling, and B. C. Sanders, "Objectively discerning autler-townes splitting from electromagnetically induced transparency," *Physical Review Letters*, vol. 107, no. 16, p. 163604, 2011.

[5] R. Lechner, C. Maier, C. Hempel, P. Jurcevic, B. P. Lanyon, T. Monz, M. Brownnutt, R. Blatt, and C. F. Roos, "Electromagnetically-induced-transparency ground-state cooling of long ion strings," *Physical Review A*, vol. 93, no. 5, p. 053401, 2016.

[6] G. Morigi, J. Eschner, and C. H. Keitel, "Ground state laser cooling using electromagnetically induced transparency," *Physical Review Letters*, vol. 85, no. 21, pp. 4458–4461, 2000.

[7] P. Lambropoulos and D. Petrosyan, *Fundamentals of Quantum Optics and Quantum Information*. Berlin; New York: Springer, 1st ed., 2007.

[8] L. Feng, W. L. Tan, A. De, A. Menon, A. Chu, G. Pagano, and C. Monroe, "Efficient ground-state cooling of large trapped-ion chains with an

electromagnetically-induced-transparency tripod scheme," *Physical Review Letters*, vol. 125, no. 5, p. 053001, 2020.